A search for charged Higgs from top quark decay at the CERN p̄p Collider

UA2 Collaboration

Bern–Cambridge–CERN–Dortmund–Heidelberg–Melbourne–Milano–Orsay (LAL)–Pavia–Perugia–Pisa–Saclay (CEN)

J. Alitti [a], G. Ambrosini [b], R. Ansari [c], D. Autiero [d], P. Bareyre [a], I.A. Bertram [e], G. Blaylock [f,1], P. Bonamy [a], K. Borer [g], M. Bourliaud [a], D. Buskulic [c], G. Carboni [d], D. Cavalli [h], V. Cavasinni [d], P. Cenci [i], J.C. Chollet [c], C. Conta [b], G. Costa [h], F. Costantini [d], L. Cozzi [h], A. Cravero [h], M. Curatolo [d], A. Dell'Acqua [b], T. DelPrete [d], R.S. DeWolf [j], L. DiLella [f], Y. Ducros [a], G.F. Egan [e], K.F. Einsweiler [f,2], B. Esposito [d], L. Fayard [c], A. Federspiel [g], R. Ferrari [b], M. Fraternali [b], D. Froidevaux [f], G. Fumagalli [b], J.M. Gaillard [c], F. Gianotti [h], O. Gildemeister [f], C. Gössling [k], V.G. Goggi [b], S. Grünendahl [ℓ], K. Hara [g,3], S. Hellman [f], J. Hrivnac [f], H. Hufnagel [k], E. Hugentobler [g], K. Hultqvist [f,4], E. Iacopini [d,5], J. Incandela [h,6], K. Jakobs [f], P. Jenni [f], E.E. Kluge [ℓ], N. Kurz [ℓ], S. Lami [d], P. Lariccia [i], M. Lefebvre [f], L. Linssen [f], M. Livan [b], P. Lubrano [f,i], C. Magneville [a], L. Malgeri [7], L. Mandelli [h], L. Mapelli [f], M. Mazzanti [h], K. Meier [f,8], B. Merkel [c], J.P. Meyer [a], M. Moniez [c], R. Moning [g], M. Morganti [d], L. Müller [g], D.J. Munday [j], M. Nessi [f], F. Nessi-Tedaldi [f], C. Onions [f], T. Pal [g], M.A. Parker [j], G. Parrour [c], F. Pastore [b], E. Pennacchio [b], J.M. Pentney [f], M. Pepe [f], L. Perini [h], C. Petridou [d], P. Petroff [c], H. Plothow-Besch [f], G. Polesello [f,b], A. Poppleton [f], K. Pretzl [g], M. Primavera [d,7], M. Punturo [i], J.P. Repellin [c], A. Rimoldi [b], M. Sacchi [b], P. Scampoli [i], J. Schacher [g], B. Schmidt [k], V. Simák [f], S.L. Singh [j], V. Sondermann [k], R. Spiwoks [k], S. Stapnes [f], C. Talamonti [i], F. Tondini [i], S.N. Tovey [e], E. Tsesmelis [k], G. Unal [c], M. Valdata-Nappi [d,7], V. Vercesi [b], A.R. Weidberg [f,9], P.S. Wells [j,10], T.O. White [j], D.R. Wood [c], S.A. Wotton [j,10], H. Zaccone [a] and A. Zylberstejn [a]

[a] Centre d'Etudes Nucléaires de Saclay, F-91191 Gif-sur-Yvette Cedex, France
[b] Dipartimento di Fisica Nucleare e Teorica, Università di Pavia and INFN, Sezione di Pavia, Via Bassi 6, I-27100 Pavia, Italy
[c] Laboratoire de l'Accélérateur Linéaire, Université de Paris-Sud, F-91405 Orsay, France
[d] Dipartimento di Fisica dell'Università di Pisa and INFN, Sezione di Pisa, Via Livornese, S. Piero a Grado, I-56100 Pisa, Italy
[e] School of Physics, University of Melbourne, Parkville 3052, Australia
[f] CERN, CH-1211 Geneva 23, Switzerland
[g] Laboratorium für Hochenergiephysik, Universität Bern, Sidlerstraße 5, CH-3012 Bern, Switzerland
[h] Dipartimento di Fisica dell'Università di Milano and INFN, Sezione di Milano, I-20133 Milan, Italy
[i] Dipartimento di Fisica dell'Università di Perugia and INFN, Sezione di Perugia, via Pascoli, I-06100 Perugia, Italy
[j] Cavendish Laboratory, University of Cambridge, Cambridge CB3 0HE, UK
[k] Lehrstuhl für Experimental Physik IV, Universität Dortmund, W-4600 Dortmund, FRG
[ℓ] Institut für Hochenergiephysik der Universität Heidelberg, Schröderstraße 90, W-6900 Heidelberg, FRG

The process t→H⁺b, H⁺→τ⁺ν, τ⁺→hadrons+ν̄ and its charge conjugate are investigated by seeking an excess in number of observed τ's beyond that expected from the standard model under the assumption of e-τ universality. No such excess is found and new regions of the m_H-m_t plane are excluded for $B(H^+ \to \tau\nu) = 0.5$ and 1.0. In addition, the ratio of couplings of the τ and e to the W is precisely measured as $g_\tau^w/g_e^w = 1.02 \pm 0.04$(stat.) ± 0.04(syst.).

1. Introduction

Little experimental information exists on the nature of the Higgs sector in the standard model (SM). The simplest extensions beyond the minimal one-doublet version are models with two doublets of complex scalar fields which imply the existence of charged Higgs bosons ($H^\pm$) [1]. In such models the $H^\pm$ couplings are fully specified by its mass, m_H, and by the ratio of vacuum expectation values for the two scalar fields, $\tan\beta = v_2/v_1$.

The existence of $H^\pm$ bosons could have important consequences for the discovery of the top quark. For $m_t > m_H + m_b$ the decay t→H⁺b competes with the standard decay t→W⁺b, where W is either virtual or on the mass shell, depending on the values of m_H and $\tan\beta$ [2]. Since in this case the dominant charged Higgs decays are H⁺→τ⁺ν, and H⁺→cs̄, with branchings which depend on $\tan\beta$ (see fig. 1 and ref. [3]), searches for the top quark based on the observation of the semileptonic decay t→be⁺ν (or t→bμ⁺ν) [4–6] would result in a much weaker signal than expected [7]. In particular, for the mass region accessible at the CERN p̄p Collider, $m_W > m_t + m_b$, the decay t→H⁺b is by far the dominant decay mode, regardless of the value of $\tan\beta$ [8]. In this case a lower
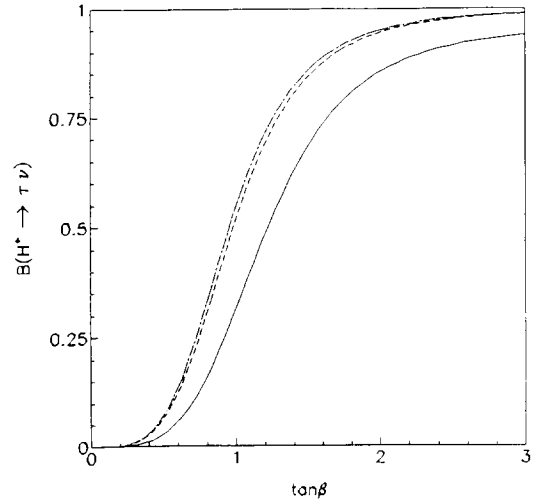

Fig. 1. $B(H^\pm \to \tau\nu)$ versus $\tan\beta$ at tree level (solid) and with QCD correction [3] for $m_t = 40$ (dashed line) and 70 GeV (dash-dotted line).

bound on the top mass can only be obtained by measurement of Γ_W [9–11] and from direct searches at LEP [12]. In this letter, we describe a search for the decay

$$t \to H^+b, \quad H^+ \to \tau^+\nu, \quad \tau^+ \to \text{hadrons} + \bar\nu, \tag{1}$$

and for its charge conjugate. The analysis method is based upon that used in the UA2 measurement of e-τ universality from W decay [13]. First, the numbers of electrons and τ's accompanied by large missing transverse momentum ($p̸_T$) are determined from the data. The number of electrons is then used together with the assumption of e-τ universality to determine the number of τ's expected from IVB decay, and this prediction can be compared with the data. A statistically significant excess of events in the data would indicate new physics whereas the agreement between data and expectation would make it possible to exclude process (1) in some regions of the model parameter space.

An earlier search for process (1) has been performed by the UA1 Collaboration [14].

[1] Present address: University of California, Santa Cruz, CA 95064, USA.
[2] Present address: Lawrence Berkeley Laboratory, Berkeley, CA 94720, USA.
[3] Present address: University of Tsukuba, Tsukuba, Ibaraki 305, Japan.
[4] Present address: University of Stockholm, S-11346 Stockholm, Sweden.
[5] Also at Scuola Normale Superiore, I-56100 Pisa, Italy.
[6] Present address: FNAL, Batavia, IL 60510, USA.
[7] Present address: Dipartimento di Fisica dell'Università della Calabria e gruppo INFN, Cosenza, Italy.
[8] Present address: Deutsches Elektronen Synchrotron, W-2000 Hamburg 52, FRG.
[9] Present address: Nuclear Physics Laboratory, University of Oxford, Oxford OX1 3RM, UK.
[10] Present address: CERN, CH-1211 Geneva 23, Switzerland.

2. The UA2 detector

The UA2 detector consists of tracking systems surrounded by calorimetry extending to within 6° of the beam axis (see ref. [15] for more details).

The central tracking detector contains two silicon pad arrays (SI) at radii of 3.5 cm and 14.5 cm used for ionization and track-point measurements [16]. A cylindrical drift chamber (JVD) [17] lies between the SI layers. Just beyond the outer SI layer are two transition radiation detectors (TRD) [18], followed by a scintillating fibre detector (SFD). The SFD [19] is made up of 18 tracking layers followed by a 1.5 radiation length (X_0) lead converter and an additional six layers of fibres used to locate the position of the electromagnetic shower initiated in the converter (preshower detector). The forward tracking detector is made up of proportional tubes (ECPT) [20] covering the pseudorapidity range $1.1 < |\eta| < 1.6$. The ECPT has six tracking layers followed by a 2 X_0 lead converter and an additional three layers of tubes. Identification of electrons in the central region relies to a large extent upon the SFD and the calorimeter (see ref. [15]).

The central calorimeter (CC) [21] covers the pseudorapidity range $-1 < \eta < 1$ while the two end cap calorimeters (EC) cover $0.9 \leqslant |\eta| \leqslant 3$. The CC is segmented into cells subtending $10°$ in polar angle θ and $15°$ in azimuthal angle ϕ. Each cell has one electromagnetic and two hadronic compartments. The end cap calorimeters are segmented into cells of size $\Delta\phi \times \Delta\eta \sim 15° \times 0.2$. All cells were initially calibrated in test beams of electrons, pions and muons. The stability of these calibrations was monitored via the response of the system to radioactive sources (^{60}Co). In the trigger and in data analysis, clusters of energy were formed in the calorimeter by joining all cells with an energy above 400 MeV which share a common edge.

The time of flight (TOF) counter system is used to select inelastic interactions produced at the time of the nominal beam crossing, thus generating a beam–beam interaction signal that defines a minimum bias (MB) event. Finally, the VETO counter array is used to identify events caused by beam–halo particles by detecting charged particles arriving before secondaries from $\bar{p}p$ interactions.

3. The selection of the data

The data used in this analysis were obtained in three major collider runs in 1988, 1989 and 1990 and correspond to an integrated luminosity of 13.0 ± 0.7 pb^{-1}. For the data from the 1988 and 1989 runs, $\not{p}_T$ triggers were used and found to be fully efficient above an offline threshold of 23 GeV and more than 96% efficient for thresholds in the range $20 < \not{p}_T < 23$ GeV. In 1990 a dedicated τ trigger was used with the goal of increasing the acceptance for $H^{\pm} \to \tau\nu$ decay (see fig. 2). At level 1 this trigger combined the $\not{p}_T$ requirement with a veto of di-jet events and a veto of events which had early VETO counter hits. The di-jet veto was obtained by running a level 1 di-jet trigger (based upon sums of transverse energy (E_T) in calorimeter cells in back to back 60° azimuthal wedges in $|\eta| < 2$) in anti-coincidence with the $\not{p}_T$ trigger. The two vetos made it possible to lower the level 1 trigger threshold by roughly 2 GeV below that of previous runs, despite the increase in peak machine luminosity.

In the offline analysis it was required that there be only one reconstructed interaction vertex and that its z coordinate (displacement along the beamline from the nominal centre of the detector) satisfy $|Z_v| < 300$ mm. To eliminate halo events it was required that there be no early veto hits. A different TOF requirement was used for the 1990 run than for the 1988 and
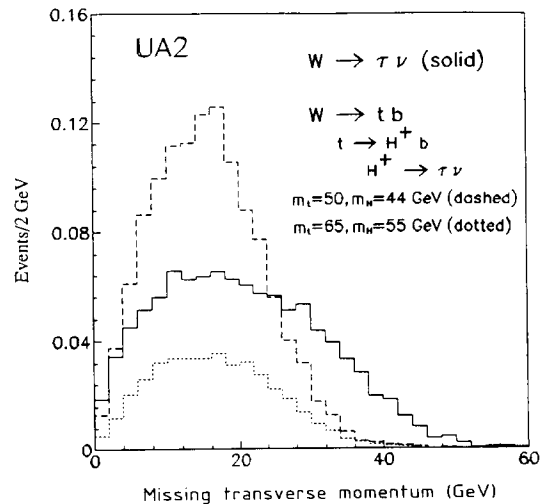

Fig. 2. Simulated $\not{p}_T$ distributions for $W \to \tau\nu$ and $H^{\pm} \to \tau\nu$ events.

1989 runs. For the latter it was required that there was no more than one early or late hit in the TOF counter, outside a window of ± 3 ns around the nominal beam crossing time. For the 1990 run it was simply required that there be no such early or late hits in order to eliminate additional background to the τ signal from beam-gas interactions. The events were then selected by requiring $\not{p}_T > 20$ GeV, $E_T^1 > 17$ GeV, where E_T^1 is the transverse energy of the leading jet in the event, and no cluster with $E_T > 10$ GeV opposite to the leading one. The τ candidates were sought on the basis of hadronicity (ξ) and profile (ρ) of the leading jet, defined as

$$\xi = E_{\mathrm{had}}/E_{\mathrm{tot}} , \qquad (2)$$

$$\rho = (E_{\mathrm{m}} + E_{\mathrm{m}}')/E_{\mathrm{tot}} , \qquad (3)$$

where E_{had} is the energy of the cluster contained in hadronic compartments, E_{tot} is the total cluster energy, E_{m} is the energy of the leading energy cell in the cluster and E_{m}' is the energy of the highest energy cell neighboring the leading cell in the cluster. Further leading cluster requirements were applied: cluster centroid in the fiducial areas of the central calorimeter cells (i.e. not within 5 mm of a crack between cells), $0.01 < \xi < 0.90$, and at least one track in a $10°$ cone around the cluster axis (defined as the line from the vertex to the centroid of the calorimeter cluster).

A subdivision of the data into "$\tau + 0$ jet" and "$\tau +$ jets" subsamples then followed according to whether an additional cluster with $E_T > 10$ GeV did or did not appear in the event. The selected samples contain the electrons from W decays, the τ's and the residual QCD jet background. In each sample the number of electrons is estimated and then most of the electron component is eliminated as described in ref. [13]. Fig. 3 shows the ρ distribution for the leading cluster for the $\tau + 0$ jet sample after rejecting the events in which the leading cluster is electromagnetic. For comparison, fig. 4 displays the ρ distributions for jets and for τ's from MC generated $W \to \tau\nu$ events after full detector simulation.

Table 1 lists the efficiencies of those cuts applied to the data which could not also be applied to Monte Carlo (MC) simulated data (discussed in the next section). The electron detection efficiencies are obtained as in the UA2 measurements of the W and Z production cross sections [9,15] except that in the
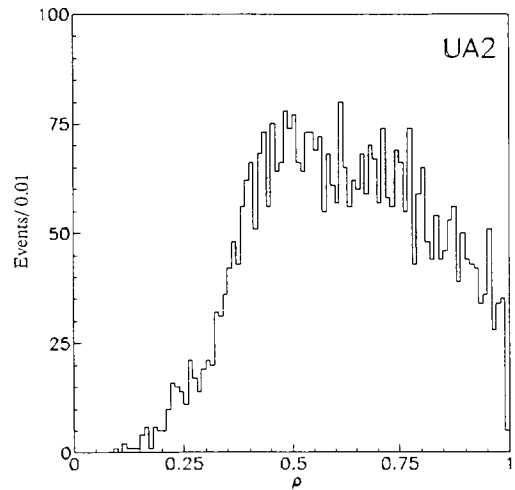

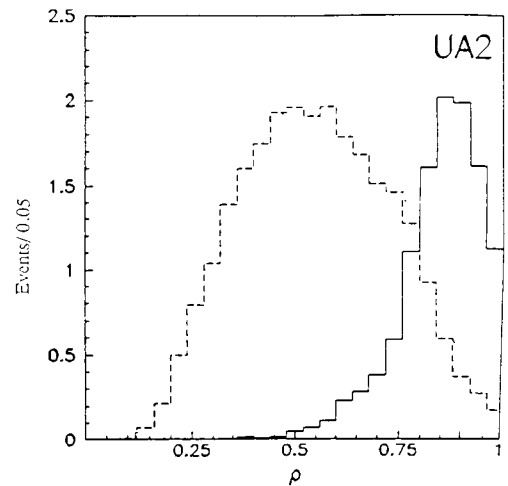Fig. 3. Cluster profile ρ distribution for the leading cluster in $\tau + 0$ jet events.

Fig. 4. Cluster profile ρ distribution for MC τ's from W decay (dashed histogram) and jets from di-jet events (solid histogram).

Table 1
Cuts applied to data only.

Cut	1988–1989 cut efficiency	1990 cut efficiency
MB	0.97 ± 0.01	0.97 ± 0.01
TOF	0.94 ± 0.01	0.80 ± 0.02
VETO	0.95 ± 0.01	0.90 ± 0.01
vertex	0.90 ± 0.01	0.81 ± 0.01

present analysis the centroid of the leading cluster was required to lie in the fiducial volume and one single vertex was required. Except for the case of TOF for which the requirement was altered, changes in efficiencies are the result of the new beam conditions in 1990. The drop in vertex efficiency, for instance, stems from the fact that there were a larger number of multi-vertex events in the higher luminosity 1990 run.

4. Determination of the τ signal

The comparison between the distributions of figs. 3 and 4 shows evidence for a τ signal in the high profile region ($\rho > 0.75$). The contaminations from halo, QCD jets and residual electrons are estimated as described in ref. [13] to determine the ratio of coupling constants g_τ^W/g_e^W. When using the thresholds given above for the $H^\pm$ search, we measure $g_\tau^W/g_e^W = 0.99 \pm 0.06 \pm 0.04$ for the $\tau + 0$ jet sample, and $g_\tau^W/g_e^W = 1.04 \pm 0.18 \pm 0.05$ for the τ+jets sample, where the first error is statistical and the second is systematical.

As an additional check, an analysis has also been performed using information from the outer silicon array. The variable used is $\delta = Q(0.5) - Q(0.1)$, where $Q(x)$ is the total signal charge in units of minimum ionizing particle equivalent (m.i.p.) measured in a cone centred on the cluster axis and of radius $x = \sqrt{\Delta\eta^2 + \Delta\phi^2}$. This quantity is a measure of the jet "narrowness" in terms of charged particles and is clearly correlated with the cluster profile. By requiring $\delta < 4.0$ m.i.p.'s, the efficiency for retaining τ's from $W \to \tau\nu$ decay is estimated to be 85% while 80% of QCD jets are rejected. The values of g_τ^W/g_τ^e obtained in this way are compatible with e–τ universality, confirming the results quoted above in the presence of a much reduced background. However, given the limited event sample, the overall uncertainty is not reduced and the following results are obtained without cutting on the value of the variable δ. Such techniques, however, may prove useful for τ studies with larger event sample as expected at future colliders.

If the event sample used is restricted to the $\tau + 0$ jet events and the $\not{p}_T$ and E_T^l thresholds are increased to 25 and 22 GeV, respectively, together with a lower

Table 2
Excess of τ's.

Sample	τ's expected	τ's observed	Excess τ's
τ+0jet	$760 \pm 31 \pm 25$	$754 \pm 68 \pm 54$	$-6 \pm 75 \pm 60$
τ+jets	$68 \pm 8 \pm 3$	$73 \pm 24 \pm 5$	$+5 \pm 25 \pm 6$

threshold of 2.5 GeV for the cluster opposite to the leading jet (thus using the same cuts as in ref. [13]), a more precise result is obtained:

$$\frac{g_\tau^W}{g_e^W} = 1.02 \pm 0.04 \,(\text{stat.}) \pm 0.04 \,(\text{syst.}) . \tag{4}$$

This result supersedes the previously published UA2 value [13].

Using the number of observed electrons and the assumption $g_\tau^W/g_e^W = 1$, estimates are obtained for the expected numbers of τ's from $W \to \tau\nu$ in the $\tau + 0$ jet and τ+jets samples, taking also into account the contribution from τ's coming from Z decays as in ref. [13]. These are then compared to the numbers of τ's observed in order to obtain the values for the τ excess given in table 2 along with their uncertainties. Note that the numbers shown in table 2 have been corrected for the efficiencies of table 1 and that the errors are computed by adding all uncertainties in quadrature. To convert the observed number of electrons into a prediction of the number of τ's from $W \to \tau\nu$, the ratio of the acceptances of τ's and electrons is used. This is calculated by MC as in ref. [13] and found to be $\Omega = 0.259 \pm 0.006$.

It is then possible to compare the τ excess with that expected if the charged Higgs hypothesis were valid.

5. Estimate of τ excess from $H^\pm \to \tau\nu$

Approximately 8000 events were generated using the programme of ref. [22] for each of 16 different choices of m_H and m_t values for both strong and weak production of top. Roughly equal-space values for the masses were chosen from the ranges $44 < m_H < 66$ GeV and $50 < m_t < 71.5$ GeV.

The estimated number of τ's expected for each case is determined after applying all the analysis cuts, except the criteria listed in table 1. The number of events remaining after the cuts is normalized via the pro-

duction cross sections for top [23], and the total integrated luminosity of 13 pb^{-1}. The effect of the τ trigger on the collection of data is taken into account by an offline simulation of all levels of the trigger when selecting events from the MC output. The expected number of events together with the acceptances (A) are listed in table 3 for $B(\mathrm{H}^{\pm} \to \tau\nu) = 1.0$. The contribution of the $t\bar{t}$ channel to the $\tau + 0$ jet sample is negligible and has not been included.

In the MC simulation τ's from $\mathrm{H}^{\pm}$ decay are generated with no polarization (contrary to the τ's from W decay, for which polarization effects are fully taken into account). As pointed out in ref. [24] the effect of τ polarization in charged Higgs decay would increase the mean momentum of the decay hadrons, thus increasing the acceptance for process (1). This effect is of about (5–10)%, as checked for $m_H = 45$ GeV, corresponding to an increase of about (2–3)% for the confidence level of the excluded region in the m_H–m_t plot (see section 7).

The analysis is also sensitive to the MC treatment of the spectator parton in the event. For this reason the MC parameters used in this analysis were obtained by comparing simulated $W \to ev$ events with real $W \to ev$ data for various MC set-ups. The key indicators used to optimize the quality of the simulation are: (i) the ratio of the number of events passing the $\tau + $jets criteria to those passing the $\tau + 0$ jet criteria, (ii) the scalar sum of transverse energy in cells of the calorimeter, and (iii) the total charge in the outer silicon layer. The data and optimized MC are found to produce distributions of these quantities which are in very good agreement.

6. Uncertainties

The systematic uncertainties in the numbers of τ's expected from W decay and of τ's observed (table 2) are to a large extent the same as those which appear in ref. [13]. The number of τ's expected from $W \to \tau\nu$ decay depends upon both τ and electron detection efficiencies. The largest single uncertainty comes from the cut in hadronicity, $\xi < 0.9$. A $\pm 5.0\%$ uncertainty is assessed for this cut by considering the difference in hadronicity values for test beam pions and electrons near calorimeter cell boundaries. The uncertainty in τ efficiency resulting from the profile cut, $\rho > 0.75$, is set at $\pm 4.0\%$ on the basis of a comparison of the profile distribution of 10 GeV pions from test beam with that of MC pions. Kinematic cuts ($\not{p}_T$ and E_T^l) have a combined uncertainty of $\pm 3.4\%$ as determined by varying thresholds in accord with uncertainties in the energy scales of the electromagnetic

Table 3
Acceptances and expected number of events from process (1).

m_t (GeV)	m_H (GeV)	$\tau + 0$ jet		$\tau +$ jets		
		A for $t\bar{b}$	expected	A for $t\bar{b}$	A for $t\bar{t}$	expected
50	44	0.007	25	0.016	0.057	118
55	45	0.015	39	0.019	0.058	92
55	49	0.027	72	0.027	0.073	125
60	45	0.019	35	0.013	0.050	44
60	50	0.046	85	0.023	0.072	70
60	54	0.058	106	0.040	0.103	113
65	45	0.015	17	0.017	0.046	31
65	50	0.044	49	0.021	0.073	41
65	55	0.088	98	0.019	0.087	42
65	59	0.114	128	0.024	0.109	52
70	45	0.010	5	0.013	0.044	14
70	50	0.034	18	0.021	0.057	21
70	55	0.085	45	0.021	0.087	25
70	60	0.149	80	0.021	0.103	28
70	64	0.169	90	0.026	0.120	33
71.5	66	0.185	79	0.025	0.122	27

($\pm 1\%$) and hadronic ($\pm 2\%$) compartments of the calorimeters. The contribution from the electrons is negligible since the central electrons from W decay are well above the E_T^1 and p_T thresholds. The uncertainty in electron identification efficiency is $\pm 1.0\%$. Using electrons from W decay the uncertainty in track efficiencies for τ's and electrons is determined to be $\pm 3\%$.

For observed τ's, the subtraction of the QCD jet background contributes a maximal uncertainty of $\pm 3.4\%$ which is evaluated by taking the difference between the ratio of the numbers of observed τ's to electrons for the case of an opposite jet E_T cut at 10 GeV and that obtained for a cut at 2.5 GeV.

There is no expected beam–halo contribution to the data sample. The uncertainty on the number of τ's resulting from the uncertainty in the halo estimate is determined as in ref. [13] to be $\pm 1\%$.

For the expected number of τ's coming from the charged Higgs channel there are contributions to the uncertainties from theoretical, MC, and experimental sources. The uncertainty in integrated luminosity ($\pm 6\%$), is included here as are the uncertainties in the number of produced top quarks. The effect of energy scale uncertainties is estimated by varying the energy thresholds. The shapes of the distributions of kinematic variables near thresholds, and consequently the τ selection efficiencies, vary with m_t and m_H between $\pm 2\%$ and $\pm 10\%$. A conservative estimate of ± 1 GeV has been added to account for the uncertainty in the low energy response of the calorimeter. The effect of this does not depend on m_H and m_t and does not exceed a variation of 10% in signal acceptance.

The uncertainty resulting from the method of reconstructing spectator parton interactions is estimated by taking the difference in signal efficiency obtained for two different MC configurations. In the first case one MB event is superimposed on the MC event in which the di-quark fragmentation of ref. [22] is included. In the second case two MB events are superimposed on the event and di-quark fragmentation is not included. This is found to be a mass-dependent effect but does not exceed $\pm 25\%$ in any of the cases considered. The effect of making reasonable variations in the b-quark fragmentation parameters [4] leads to a variation in signal which does not exceed $\pm 8\%$ for any of the cases studied.

In the case of mass dependent uncertainties, the maximum uncertainties mentioned above are used.

7. Excluded regions in the m_H–m_t plane

Having estimated the contributions to the uncertainties in the observed τ excesses in the $\tau + 0$ jet and τ+jets samples as well as the mass-dependent τ excess expected for $H^\pm$ decays, it is possible to ask whether the observations, consistent with zero τ excess, are sufficient to exclude the existence of $H^\pm$ for some values of the parameters. For this purpose, levels of confidence for the exclusion of the decay (1) for each of the 16 mass sets used in the MC, and for values of the branching ratio $B(H^\pm \to \tau\nu)$ (B) of 0.5 and 1.0, were calculated.

For a given data sample and set of parameter values, the various statistical and systematic uncertainties in the numbers of observed and expected τ's are combined into a single uncertainty, using a MC programme which takes into account the shapes of the uncertainty distributions and known correlations between uncertainties. For both samples the probability of observing a τ excess smaller than the one listed in table 3 is computed for each pair of masses (m_H–m_t) and corresponds to the confidence level (CL) for exclusion of the $H^\pm$ hypothesis. The error distribution obtained with the MC programme is found to be approximately gaussian. For the $\tau + 0$ jet sample the error is dominated by the statistical uncertainty whereas for the τ+jets sample the statistical and systematic uncertainties are of similar size.

The CL's for the exclusion of the 16 points considered are given in table 4 for B values of 1.0 and 0.5. These correspond to tan β values above roughly 2.0 and 1.0, respectively, as determined after a QCD correction [3]. Also shown in table 4 are the CL's for the weighted mean combination of the two samples. By interpolating the CL's for the 16 mass points, it is possible to define regions of the m_H–m_t plane which are excluded at 90% and 95% CL. These are shown in figs. 5 and 6.

The regions excluded by UA1 [14] are also shown as are the model independent lower bounds for m_t from hadron collider measurements of Γ_W [9–11] and m_H from LEP [25].

Table 4
Exclusion confidence levels (%).

m_t (GeV)	m_H (GeV)	$B=1$			$B=0.5$		
		$\tau+0$ jet	$\tau+$jets	all	$\tau+0$ jet	$\tau+$jets	all
50	44	60.7	99.9	99.9	55.7	92.5	92.6
55	45	65.4	99.4	99.5	58.1	88.2	88.5
55	49	76.4	99.9	99.9	64.3	92.9	93.5
60	45	64.2	91.9	92.6	57.5	72.8	73.7
60	50	79.8	98.4	98.9	66.5	83.9	85.9
60	54	85.0	99.9	99.9	70.1	92.6	93.8
65	45	57.5	83.1	83.5	54.1	64.8	65.3
65	50	69.1	90.6	92.0	60.2	71.3	73.0
65	55	83.0	91.1	95.0	68.6	71.9	77.3
65	59	89.3	95.4	98.2	73.5	77.3	83.4
70	45	52.8	63.2	63.4	51.7	52.7	52.9
70	50	57.8	72.5	73.5	54.2	57.8	58.6
70	55	68.1	77.9	81.5	59.6	61.3	64.1
70	60	78.6	80.6	87.8	65.7	63.0	69.4
70	64	81.4	84.7	91.2	67.5	66.1	72.7
71.5	66	78.7	79.3	87.2	65.8	62.2	68.9
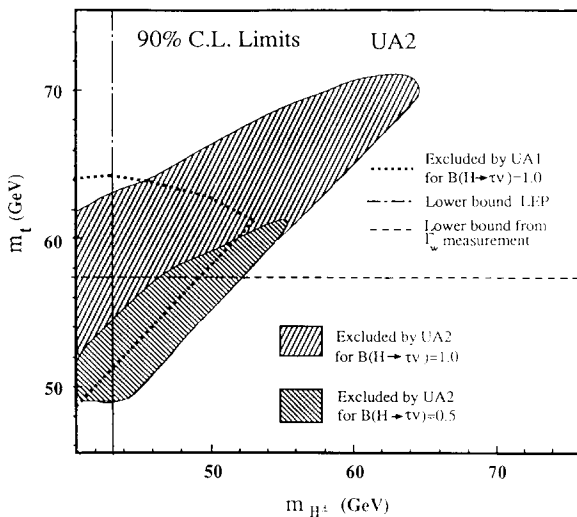
Fig. 5. Regions of the m_H–m_t plane excluded at 90% CL; the LEP bound is for $B=1$, 95% CL.
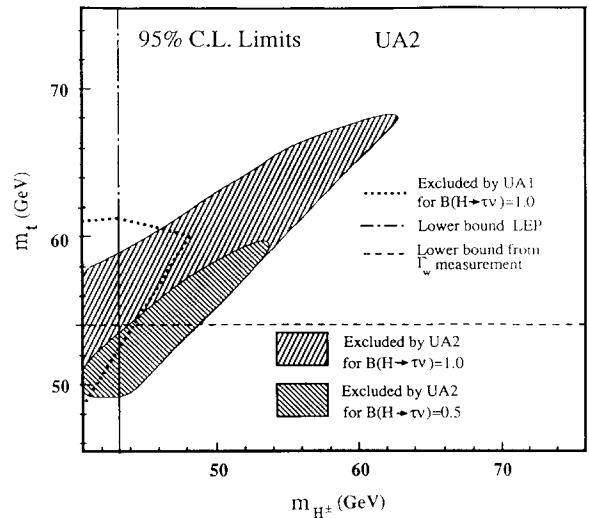

Fig. 6. Regions of the m_H–m_t plane excluded at 95% CL; the LEP bound is for $B=1$, 95% CL.

8. Conclusions

Hadronic τ decays and electrons have been counted in a sample of events with high missing transverse momentum obtained with the UA2 apparatus. The data sample corresponds to an integrated luminosity of 13.0 ± 0.7 pb^{-1} at $\sqrt{s}=630$ GeV. No excess in the number of τ's beyond the number expected from IVB decays is observed allowing the decay chain

$$t \rightarrow H^+ b, \; H^+ \rightarrow \tau^+ \nu, \; \tau^+ \rightarrow \text{hadrons} + \bar{\nu}$$

to be excluded in new regions of the m_H–m_t plane for $B(H^\pm \rightarrow \tau \nu)$ values of 0.5 and 1.0. In addition, the

ratio of couplings of the τ and electron to the W is measured to be

$$\frac{g_\tau^W}{g_e^W} = 1.02 \pm 0.04 \pm 0.04 ,$$

which is consistent with e–τ universality.

Acknowledgement

References

[1] J.F. Gunion et al., The Higgs hunter guide (Addison-Wesley, New York, 1990).

[2] S.L. Glashow and E. Jenkins, Phys. Lett. B 196 (1987) 233.

[3] M. Drees and D.P. Roy, CERN preprint CERN-TH 6080/91 (April 1991).

[4] UA2 Collab., J. Alitti et al., Z. Phys. C 46 (1990) 179.

[5] CDF Collab., F. Abe et al., preprint FERMILAB Pub 90-137 E.

[6] UA1 Collab., C. Albajar et al., Z. Phys. C 48 (1990) 1.

[7] A.S. Joshipura and S.D. Rindani, Mod. Phys. Lett. A 6 (1991) 3375.

[8] V. Barger and R.J.N. Phillips, Phys. Rev. D 41 (1990) 884.

[9] UA2 Collab., J. Alitti et al., Phys. Lett. B 276 (1992) 365.

[10] CDF Collab., F. Abe et al., Phys. Rev. D 44 (1991) 29.

[11] UA1 Collab., C. Albajar et al., Phys. Lett. B 253 (1991) 503.

[12] ALEPH Collab., D. Decamp et al., Phys. Lett. B 236 (1990) 511;
DELPHI Collab., P. Aarnio et al., Phys. Lett. B 242 (1990) 542;
OPAL Collab., M.Z. Akrawy et al., Phys. Lett. B 236 (1990) 364.

[13] UA2 Collab., J. Alitti et al., Z. Phys. C 52 (1991) 209.

[14] UA1 Collab., C. Albajar et al., Phys. Lett. B 257 (1991) 459.

[15] UA2 Collab., J. Alitti et al., Z. Phys. C 47 (1990) 11.

[16] R. Ansari et al., Nucl. Instrum. Methods A 279 (1989) 388.

[17] F. Bosi et al., Nucl. Instrum. Methods A 283 (1989) 532.

[18] R. Ansari et al., Nucl. Instrum. Methods A 263 (1988) 51.

[19] R. Ansorge et al., Nucl. Instrum. Methods A 265 (1988) 33;
J. Alitti et al., Nucl. Instrum. Methods A 279 (1989) 364.

[20] K. Borer et al., Nucl. Instrum. Methods A 286 (1990) 128.

[21] A. Beer et al., Nucl. Instrum. Methods A 224 (1984) 360.

[22] H. Bengtsson, Comput. Phys. Commun. 31 (1984) 323;
H. Bengtsson and T. Sjöstrand, Comput. Phys. Commun. 46 (1987) 43;
T. Sjöstrand, Intern. J. Mod. Phys. 3 (1988) 751.

[23] T. Altarelli et al., Nucl. Phys. B 308 (1988) 724.

[24] D.P. Roy, CERN preprint CERN-TH 6274/91 (October 1991);
B.K. Bullock, K. Hagiwara and A.D. Martin, Phys. Rev. Lett. 67 (1991) 3055.

[25] ALEPH Collab., D. Decamp et al., Phys. Lett. B 241 (1990) 623;
DELPHI Collab., P. Abrew et al., Phys. Lett. B 241 (1990) 449;
L3 Collab., B. Adeva et al., Phys. Lett. B 252 (1990) 511;
OPAL Collab., M.Z. Akrawy et al., Phys. Lett. B 242 (1990) 299.